The Dynamic Response and Evaluation of a Flare Storage Container during Slow Cook-off using Abaqus Explicit – CEL

P. Carlucci[1], J. Jablonski[1], A. Colletti[1], T. Heithoff[1] and J. P. Granuzzo[1]

[1]U.S. Army – ARDEC, Picatinny Arsenal, Picatinny, NJ 07806

Abstract: Sealable ammunition containers are widely used by the U.S. Army to ensure safe transport and storage of various types of munitions for the warfighter. In the case of accidental ignition, ammunition containers are designed to fail in a way that minimizes danger to nearby personnel. In the constant effort to improve the performance and safety of such containers, extensive experimental testing is required to assess new or modified designs. This testing is time-consuming, costly, and often yields only pass/fail results with little or no data for failure analysis. Recent efforts were taken to apply modeling and simulation to down-select design concepts and help focus testing efforts for these designs. The M548 ammunition container is used to store up to twenty-four signal flares. Structural response of the container during slow cook-off was modeled using the Coupled Eulerian-Lagrangian (CEL) capability in Abaqus/Explicit. Comparison was made between the original configuration and a proposed venting re-design. Simulation results indicate the re-design performs better, as well as confirming the observed test results of the original.

Keywords: fluid-structure interaction, compressible inviscid flow, Noble-Abel gas, propellant combustion, closed bomb, safety, structural dynamics, explicit, CEL, ammunition container.

1. Background

1.1 Overview

Abaqus Explicit with Coupled Eulerian-Lagrangian (CEL) has the capability to define nodes which are able to generate mass at a defined temperature during a simulation. These are referred to as inflator nodes and were initially intended to allow the automotive industry to simulate air bag deployment. Inflator nodes can be arbitrarily located in space, irrespective of the Eulerian mesh. Wherever an inflator node is located within an Eulerian element, an associated mass is introduced into the element as a point source. The authors refer to these elements (Eulerian elements with internal inflator nodes) as inflator elements, though the elements which contain inflator nodes can change arbitrarily during an analysis. The mass generation rate of an inflator node can be defined as a function of the pressure acting on its corresponding inflator element through the use of user subroutines.

1.2 Theory of Inflator Nodes

The governing Navier-Stokes equations for a compressible inviscid flow that account for the behavior of inflator nodes can be written in conservation form as follows:

Continuity Equation:

$$\left(\frac{\partial \rho}{\partial t} + \frac{\partial \rho}{\partial t}\Big|_{inf}\right) + \nabla \cdot (\rho \vec{\boldsymbol{v}}) = 0 \qquad \textit{EQ-1}$$

Momentum Equation:

$$\frac{\partial}{\partial t}(\rho \vec{\boldsymbol{v}}) + \nabla \cdot (\rho \vec{\boldsymbol{v}} \vec{\boldsymbol{v}}) = \rho \vec{\boldsymbol{f}} - \nabla p \qquad \textit{EQ-2}$$

Energy Equation:

$$\frac{\partial}{\partial t}\left[\rho\left(e + \frac{v^2}{2} + e_{inf}\right)\right] + \nabla \cdot \left[\rho\left(e + \frac{v^2}{2}\right)\vec{\boldsymbol{v}}\right] = \rho \dot{q} - \nabla \cdot (\rho \vec{\boldsymbol{v}}) + \rho \vec{\boldsymbol{f}} \cdot \vec{\boldsymbol{v}} \qquad \textit{EQ-3}$$

As can be seen from (EQ-1), an inflator node adds a mass source term to the continuity equation. This generation term is lumped with unsteady density fluctuations within the control volume and is not correlated to the mass flux through the control surface. As a result of this modeling assumption, the momentum equation (EQ-2) remains unchanged. However, the generation of mass within the control volume also leads to an additional energy term coupled with the unsteady energy fluctuations within the control volume as seen in the energy equation (EQ-3). Present implementation of inflator nodes assumes that the mass generated within the control volume entered through some virtual boundary (i.e. boundary works was required) and thus its corresponding energy addition can be expressed in terms of enthalpy. Thus, the following relation (EQ-4) can be established.

$$e_{inf} = c_p T_{inf} \qquad \textit{EQ-4}$$

In essence, mass generation is treated as an external flow into the inflator element through the inflator node. In this respect, the inflator node is treated as a boundary of an open system. Schematically, the function of an inflator node within an Eulerian element is shown in Figure 1.

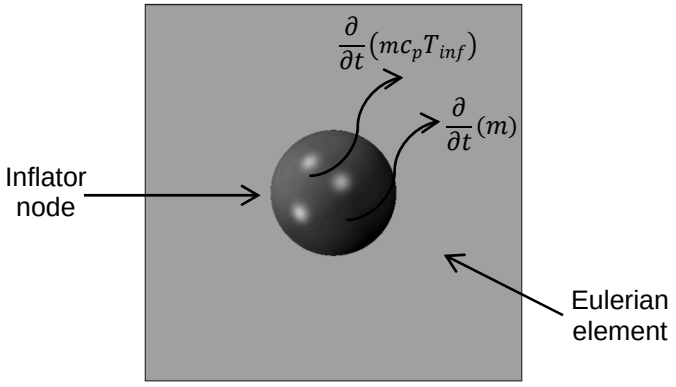

Figure 1. Schematic function of an inflator node

In order for the propellant gas generation to be modeled correctly, it is important that the volume occupied by the inflator elements is at least the same order of (or larger than) the volume occupied by the actual granular propellant. If this is not done, the flow out of an inflator element can become choked, which results in inaccurately higher pressure acting on the element. Since the propellant burn rate is dependent on pressure, such an effect causes artificially high gas generation. This criterion gives the basis for selecting the number of inflator nodes needed.

Previous efforts demonstrated that inflator elements were a viable candidate to couple propellant combustion models into Abaqus. Essentially, an inflator node can be used to abstractly represent solid propellant and simulate the introduction of gaseous propellant (as it burns from its solid state) into the Eulerian domain of the model. This allows the gas dynamics of propellant combustion to be incorporated into a structural code without directly modeling the grains of propellant (a task that is computationally infeasible for practical problems). Through the utilization of user subroutines, pressure dependent propellant models were integrated to govern the mass generation rate of inflator nodes. It is important to note that in this approach, the solid propellant is not modeled and, consequently, the interplay between the propellant gas dynamics and the structural response of the solid propellant is neglected. However, in many practical applications this effect is negligible.

1.3 Inflator User Subroutine

For inflator elements to be useful in coupling propellant combustion models with structural codes there must be flexibility in defining their mass flow rate behavior. This is accomplished through a user subroutine to interface with inflator nodes. It provides a construct which naturally divides the FEA structural code and the internal ballistics calculations. As such, the Abaqus solver allows the subroutine to compute a different mass flow rate for each inflator node at every time increment. Additionally, the stress present at each inflator element (which can be used to determine the hydrostatic pressure acting on an element) is provided to the subroutine to determine the updated burn rate based on the current element pressure.

For the propellant being considered, the linear burn rate can be assumed to take the form of equation (EQ-5). Both A and n are experimentally determined constants for each propellant, making burn rate dependent only on the current pressure, p.

$$\beta = Ap^n \qquad EQ\text{-}5$$

The subroutine is responsible for the computing and storing of all solid propellant parameters (material properties, geometry, etc.) Conceptually, the subroutine-to-Abaqus interaction is easy to understand. When called for a particular inflator element, the subroutine is given the stresses acting on the element and thus, the pressure. From this pressure, the linear burn rate can be calculated. The subroutine then determines how much surface regression will occur for all the grains in a given element. With this known, the mass flow rate for the inflator element can be calculated and sent back to the Abaqus solver. Since the subroutine internally keeps track of how much propellant has burned, it can determine when burnout occurs and will force an inflator node to cease generating mass.

2. Model Definition

2.1 Problem Description

The M548 ammunition container is used to store a wide variety of munitions. For the analyses considered here, it was modeled in its configuration for storing twenty-four signal flares. The approximate outside dimensions of the container are 425 mm x 200 mm x 350 mm, with a photo in its typical field setting shown in Figure 2 below.

Figure 2. U.S. Army M548 Ammunition Storage Container

The response of the container under slow cook-off conditions, such as a fire, when propellant ignition occurs in the signal flares was examined. Specifically, the analyses were to determine how well the main structure of the container was able to contain the internal components once the propellant ignites and burns. At the start of the analysis, it was assumed that all the propellant present in all the flares is uniformly ignited. For purposes of simplification, the pyrotechnic material in the flares is assumed not to react during the timescale that the propellant burning (since it is mechanically separated by metal parts and a delay column).

Two designs were considered for comparison which included the original unvented design as shown in Figure 2, as well as a proposed design with 170 mm x 80 mm cutouts centered on both of the largest faces of the container as shown in Figure 3 adjacent to the original design. In the proposed design, the cutouts would be sealed with a low melt temperature material that would allow them to melt at the onset of cook-off. Once ignition of the propellant occurred, the cutouts would be unobstructed allowing free venting of the container and thus the window is open at the start of the analysis.

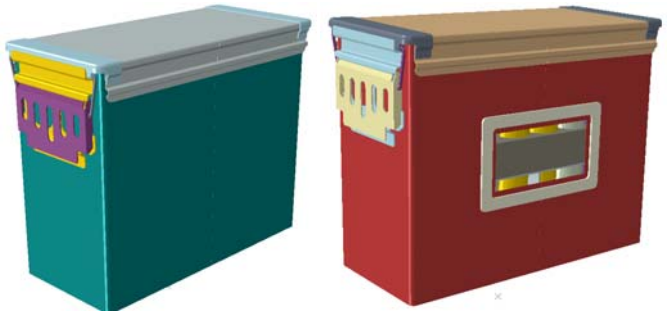

Figure 3. U.S. Army M548 Ammunition Storage Container original and proposed design with vents

Individual flares are packed in polymer tubes, which are then packed into the M548 with foam and a spacer bracket. Figure 4 shows a cut away view of the flare as well as the packing media inside the M548 container.

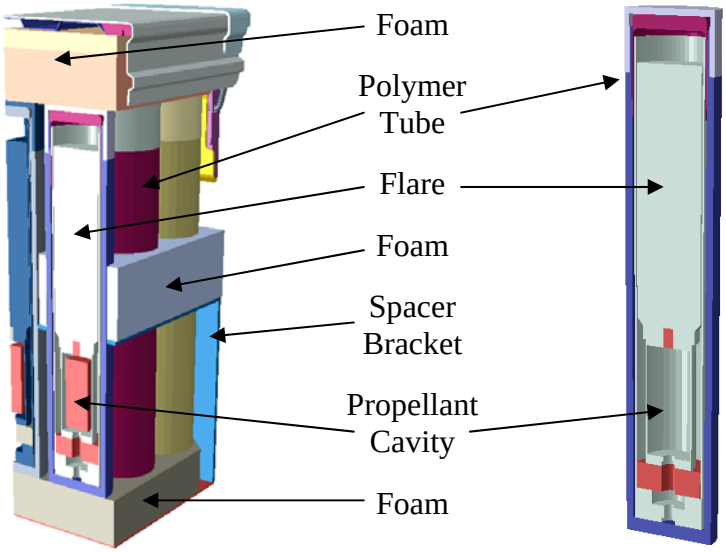

Figure 4. U.S. Army M548 Ammunition Storage Container packing media and flare

2.2 Model

The geometry allowed the analysis to be modeled using one-quarter symmetry, which greatly reduced the required computational overhead. Additional computational cost was saved in modeling the container and tube walls using SC8R continuum shell elements (~50,000 total), but ~ 300,000 C3D8R brick elements were still required to model the remainder of the lagrange components. A very fine mesh was required for the Eulerian domain, ~550,000 EC3D8R elements, in order to correctly resolve the contact between the container walls and the propellant gases. The total element count approached one million.

A moving Eulerian mesh domain was also employed in this model to help reduce the computational expense. The initial bounds of the Eulerian domain were maintained close to the Lagrange parts for the container body and cover, and the faces of the Eulerian domain were set up to track the motion of these Lagrange parts. Figure 5 shows how the domain was able to follow the motion and expand accordingly. An additional benefit of this approach was that it allowed for a relatively fine initial mesh, especially in the region of the inflator nodes, which then expanded along with the evolving propellant gases.

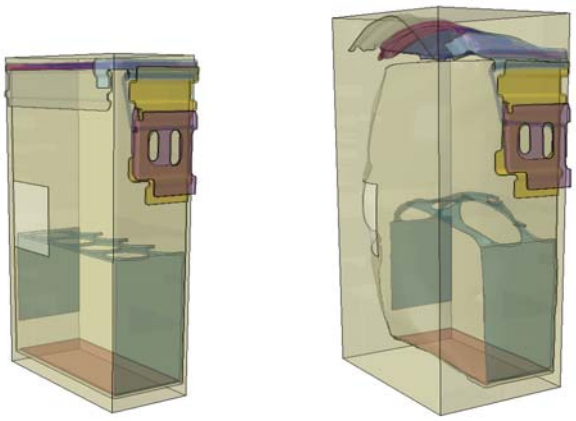

Figure 5. Moving Eulerian Mesh Domain, at start (left) and end (right) of analysis

A total of 11,000 inflator nodes were defined and evenly distributed in the interior cavities of the signal flares, as shown in Figure 6. From a modeling standpoint, this abstracted the 23 grams of granular propellant per flare as a collection of nodes located in the propellant cavity. Which were located to occupy the approximate volume of the packed propellant volume.

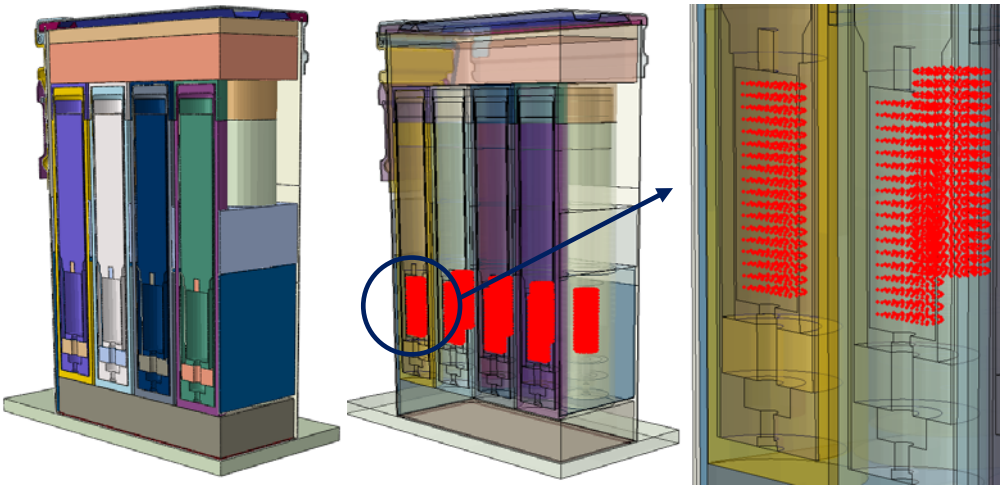

Figure 6. Location of inflator nodes in the Eulerian domain (highlighted red)

3. Analysis Results

3.1 Initial rupture of flare tube

When ignition begins at analysis start, the propellant represented by the inflator nodes begins generating propellant product gases at the first analysis increment. This gas is fully contained within the propellant cavity inside the flare, and would normally exit via the nozzle to launch the flare. Since these flares are held captive inside their storage tubes, the evolving product gases cannot escape. When the internal pressure becomes high enough, the flare tube ruptures and the product gases begin filling the main storage container. This initial evolution is depicted in Figures 7 and 8, up to rupture of the polymer tube.

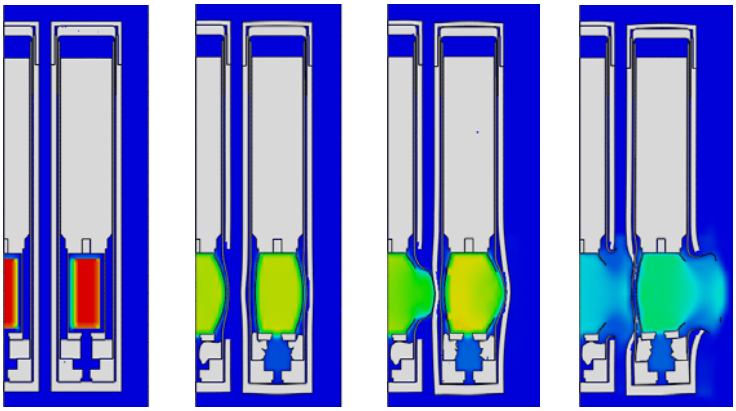

Figure 7. Pressure Contours leading to initial rupture, flares along centerline

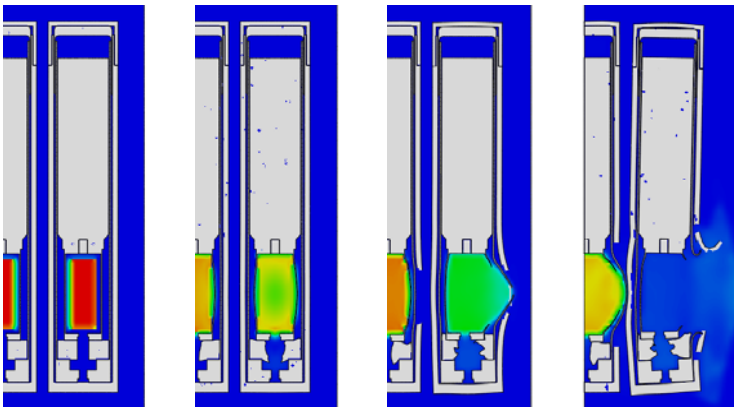

Figure 8. Pressure Contours leading to initial rupture, flares off centerline

It was initially expected that all the flares would rupture at almost the same time. The analysis shows that in actuality the tubes closest to the container wall rupture first probably due to

early interaction of the bulging tubes and container, as well as asymmetries from the geometry and mesh. This is especially pronounced between flares located along the outer walls and those fully confined by other flares.

3.2 Evolution of propellant gases into the storage container

Once individual flares begin rupturing propellant product gases quickly begin filling the main container. This rapid venting of gas inside the container leads to very large displacements of the main walls, as well as the flares themselves. Figure 9 shows four temporal snapshots of this process.

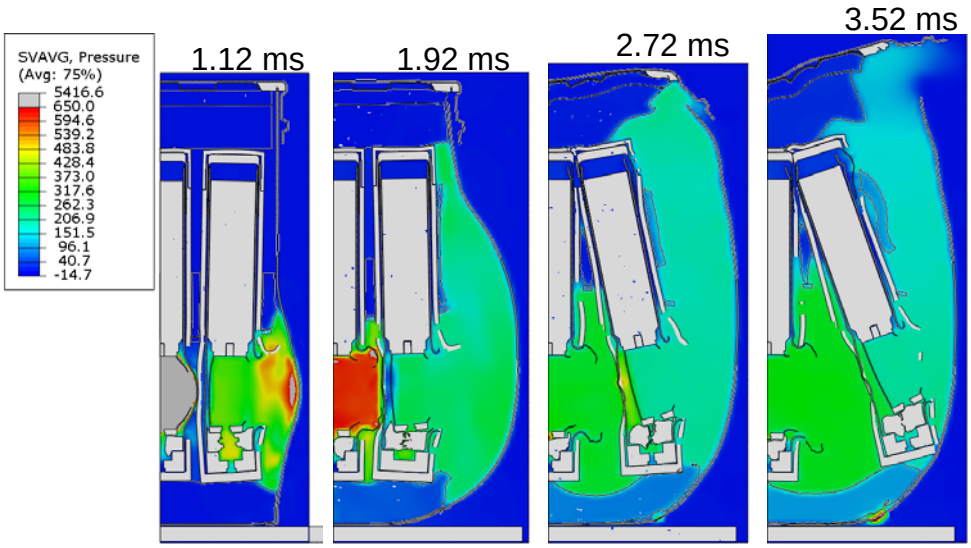

Figure 9. Pressure Contours in the original M548 container after flare rupture (psi)

The rupture and venting of the flares occurs so quickly that the container is slow to respond (due to the highly coupled nature of burning propellant to local pressure). By the time the top cover deforms enough to allow venting to the atmosphere, the container and contents have undergone extensive deformation and damage. Also of note is that the product gases become trapped between the inside rows of flares, as seen in Figure 9 in the last two time frames. The close packing distance of the flares, along with the packing foam and spacer is the underlying cause of this. This local high pressure is two to three times greater than the pressure on the opposite side of the flare, and will likely lead to internal components being expelled at very high velocities.

3.3 Comparison of original versus vented design

Once a baseline analysis for the original design was complete, a new iteration for the proposed design with an open vent was completed. Initially it was thought that a pressure time history could be monitored at a prescribed location in the container, with these histories compared to assess the effectiveness of the new design. It became apparent when viewing the results that the internal interactions were much more complicated than anticipated, and a comparison of pressure

time histories would not accurately depict the differences in the designs. After reviewing the results of the analyses, it was decided that pressure contours would be best to evaluate the designs. Figures 10 and 11 below shows the pressure contours at 2.4 ms for both designs at four different cross sectional slices (located through the flares).

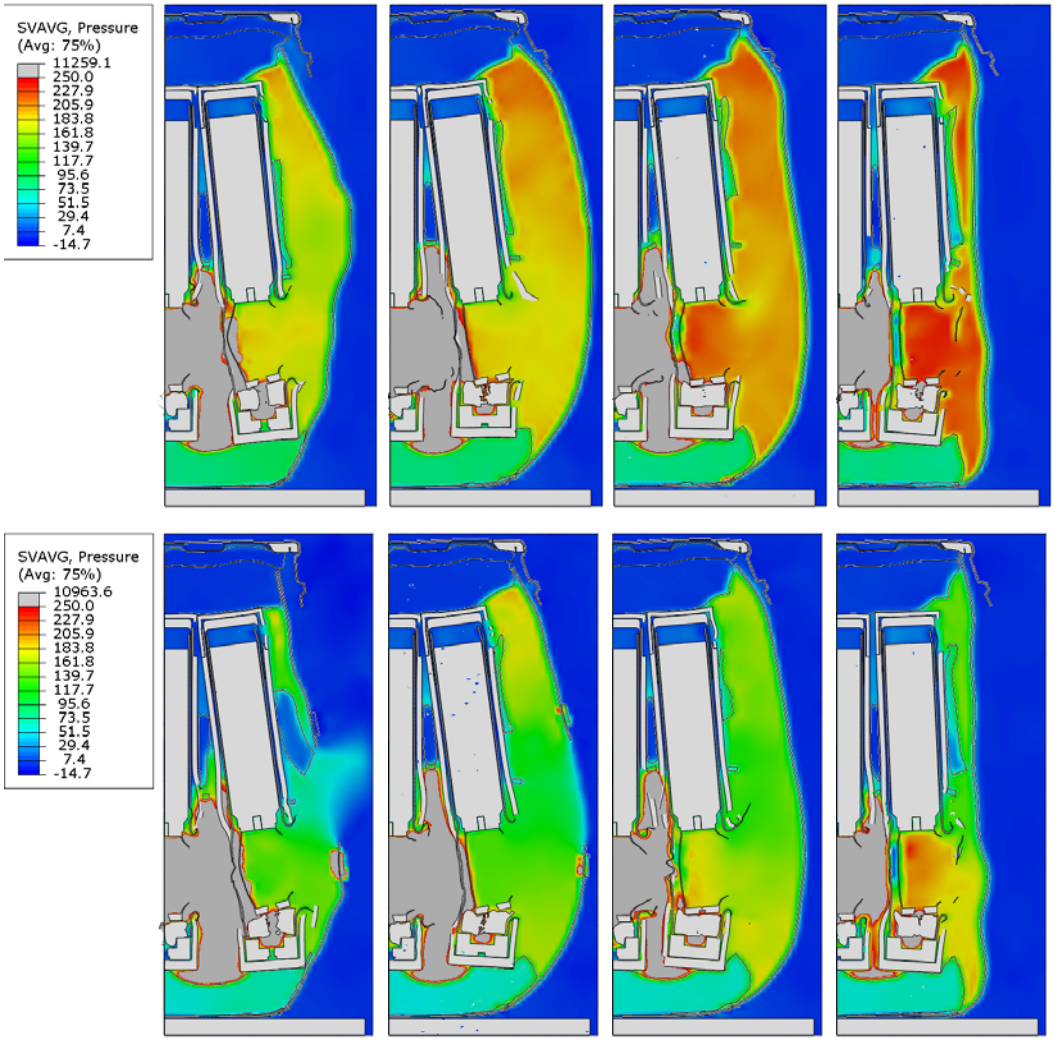

Figure 10. Pressure Contour comparison, Top Original, Bottom venting design at 2.4 ms, Contour maximum value 250 (psi)

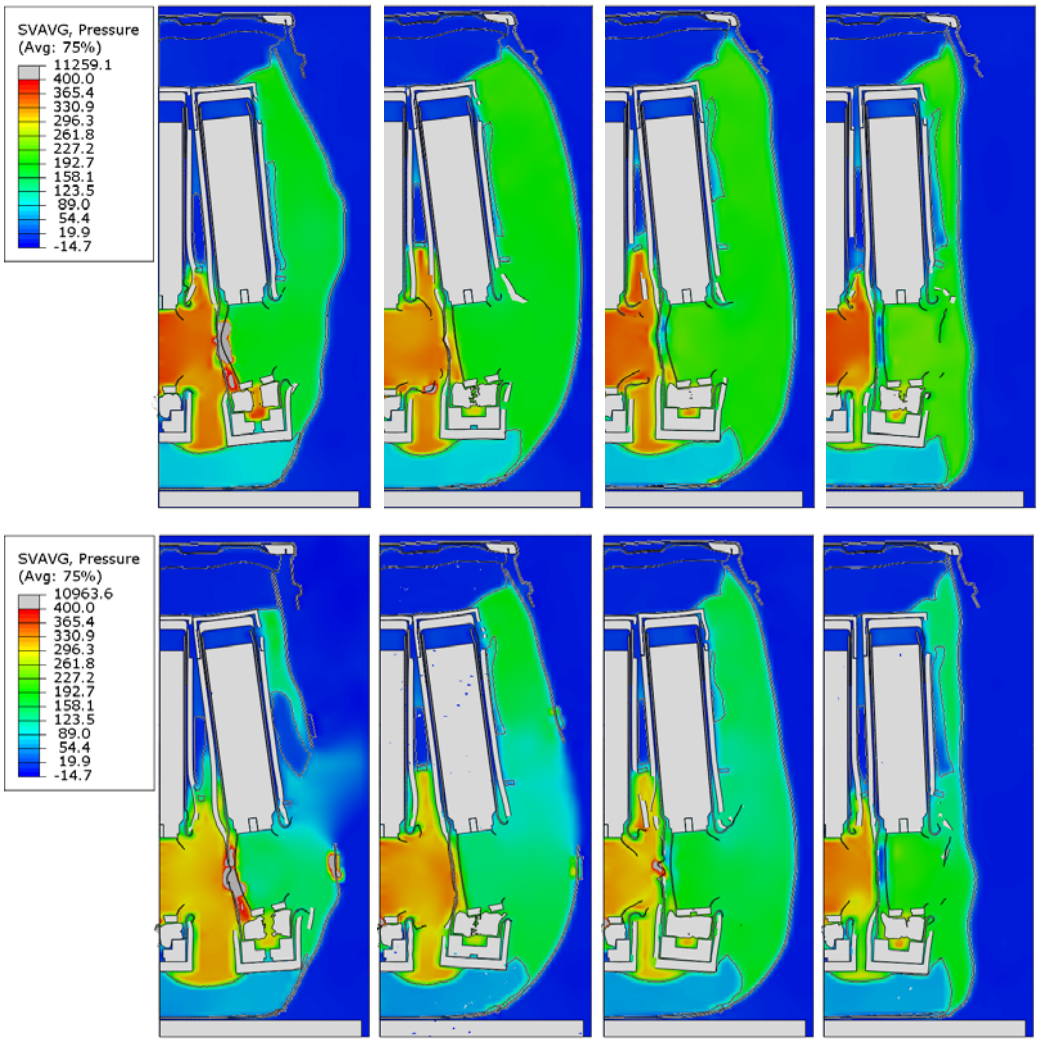

Figure 11. Pressure Contour comparison, Top Original, Bottom venting design at 2.4 ms, Contour maximum value 400 (psi)

As expected, the vented design is fairly effective at reducing the pressure acting directly on the container wall, reducing this pressure by about a factor of two. From the contour plots it is clear that the product gas generation rate is still large enough to choke the flow, since the pressure is still relatively large inside the container. The pressures between the flares are still quite high for the vented design, with only about a 25% reduction in pressure as compared to the original design. Clearly the packing materials play a significant role in the venting process.

4. Discussion

4.1 Venting the container

When considering an open vent design, it is necessary for the container to have appropriately sized vents. If the area of the vent is too small, the gaseous products generated from the solid propellant combustion will choke the flow (be produced at a greater rate than they can flow through the vent). This will lead to a pressure increase in the container and, since the burn rate is pressure dependent, the rate of gas production will accelerate. As a result the propellant may enter a runaway reaction and cause a catastrophic failure of the container. However, it is also not acceptable to make the vent arbitrarily large as this will begin to affect the structural integrity of the container, compromising its robustness. In essence, sizing the vent becomes an optimization problem.

In this case, the packing material as well as the spacing of the flares plays a significant role in the venting process. While the proposed vent window makes a significant reduction on the pressure acting on the container, a large amount of the product gases remain trapped between the cavities between the flares. The pressures in these cavities increase rapidly leading to larger burn rates in a runaway progression. The valuable insight from these analyses makes it clear that a more comprehensive approach may be necessary to effectively vent under cook-off conditions.

4.2 Analysis challenges

At this time it is necessary to discuss some of the challenges encountered in running this analysis. As is likely apparent to the reader from the previous figures and discussion, the components in the flare storage container undergo very large deformations, and are being loaded well beyond their yield strength. In fact, it is likely that mainly the inertia of the components is what is restricting the venting of the product gases. For these reasons, getting the analyses to run without numerical errors was very difficult. Fortunately, features in Abaqus such as distortion control and element deletion could be used to run the analysis as far out as possible. Despite this, the authors could not run the analyses are far out as we would have liked. Surprisingly, the proposed design with the vent window in place proved to be more difficult to run longer than the original design. The limiting factor was due to a steadily decreasing time-step in the Eulerian domain, likely due to the large pressure/density gradients in the venting gases though further investigation is planned.

5. Conclusions

In simulating the ignition of propellants inside of a sealed container, it is clear that incorporating the fluid-structure interaction of the produced gases with burn models for the propellant is necessary for an accurate analysis. It has been demonstrated that the present capabilities of Abaqus Explicit – CEL are sufficient to accurately incorporate the required physics of this process into a finite element model. Therefore, Abaqus can be used as a predictive tool in the design of sealed containers that are packaged with pyrotechnics, or other combustible products. This modeling capability has great potential for packaging engineers in the military and

commercial sectors. Due to the complexity and highly coupled nature of the physics involved in these types of events, there exists a substantial knowledge gap in packaging engineering. As a result, much information relating to a package design is inferred qualitatively through costly testing. It is hoped that the insights provided by using Abaqus as a research tool will bridge this gap.

In the case of the M548 container, the results of these analyses have provided valuable insight. While it is intuitive that a venting window will help, previously there was no practical way to estimate the effectiveness without experimental testing. In addition, this work highlighted the significant role that the internal packaging materials played in the venting response. This complex interaction could not be readily discerned from testing. The analysis results were successful in helping focus the direction of future designs of venting schemes for mitigating danger for slow cook-off events.

6. References

1. Abaqus Users Manual, Version 6.11-1, Dassault Systemes Simulia Corp., Providence, RI.
2. Anderson, J. D., "Modern Compressible Flow with Historical Perspective, Third Edition", McGraw Hill, 2003
3. Anderson, R., D. and Fickie K. D., 1987: IBHVG2 – A User's Guide, US Army Ballistic Research Laboratory Technical Report BRL-TR-2829, Aberdeen Proving Ground, MD.
4. Carlucci, D. and Jacobson S., 2008: Ballistics, Theory and Design of Guns and Ammunition, CRC Press, Boca Raton, FL.
5. Jablonski, J., Carlucci, P., Ingerick, C., 2011: Modeling the Commbustion of Pyrotechnic Materials inside Sealable Ammunition Containers Using Abaqus/Explicit-CEL, 2011 Simulia Customer Conference Proceedings, Barcelona, Spain.
6. Jablonski, J., Carlucci, P., Carlucci, D., Arata, J., Ji, H., "A Novel Approach in Coupling Interior Ballistic Models to Finite Element Codes" 27th Army Science Conference Proceedings, Orlando, FL, Nov 29 – Dec 2 2010.
7. Robbins, F., 2002: Interior Ballistics Course Notes, Self published, Aberdeen, MD.